A global method of generating action potentials and EEG oscillations in a topological surface network

Model Predictions and Speculations

Siddhartha Sen (Email: sen1941@gmail.com)
Centre for Research in Adaptive Nanostructures and Nanodevices,
School of Physics, Trinity College Dublin, Ireland

Acknowledgment

I would like to thank Samik Sen for producing all the EEG waveform Gnuplots. Mike Coey, for encouragement, Tomas Ryan and Maurizio Pezzoli for numerous discussions, Maurizio Pezzoli for producing the illustrative figures, Arnab Das for his interest, and David Muldowney for reading through and commenting on an earlier version of this work. This research did not receive any specific grant from funding agencies in the public, commercial or not-for-profit sector.

Abstract

In this paper we complete a project to demonstrates that both action potential like and EEG waveform like brain excitations can be viewed as excitations generated by exploiting the topological connectivity properties of the brain, thereby relating function to form. This is done by first proving that it is possible to find a two dimensional mathematical surface network that exactly captures the topological architecture of any hypothetical brain connectome. It is then suggested that such a surface can be taken to be a mathematical representation of the brain if it is charged and if it has surface spin half particles as then it can be shown that the surface can generate a variety of one dimensional action potential like soliton voltage pulse signals and co-producing two dimension surface EEG like waveforms in responds to local surface pinch deformations input signals. The charged soliton pulses found are shown to carry details of the input signals deformation parameters that create them and can transfer this information to the pathways they traverse as a helical non transient topologically stable alignment of surface spins: a memory substrate. The substrate has a natural, theoretically determined, excitation frequency that can be used to retrieve memories by resonance . In an earlier work soliton pulse generation and memory creation stability issues were discussed. Here we show how EEG like excitations are co-produced and establish their properties. We determine the analytic expressions, of EEG waveforms, determine their frequencies, show that frequencies are inversely relate to the waveform amplitudes, and related to symmetric tiling of a sphere and show how they are modulated by other signals. As an example we describe how the scheme can be used to explain the complex sequence of EEG excitations observed in deep sleep. We speculate on how action potentials and EEG waveforms cooperate to retrieve memory and help to focus attention.

keywords: memory retrieval, solitons , transient excitations, surface waveforms, K-complexes, sleep-spindles, sharp-wave ripples, attention.

Introduction

In this paper we complete a project to show how all observed brain excitations can be produced by exploiting the complex topological connectivity properties of the brain. In an earlier paper (Sen,2021)it was shown that action potential like one dimensional soliton voltage pulse excitations could be created in a surface network that has a topological architecture that exactly captures the topology connectivity of any hypothetical brain connectome. It was shown that exact analytic forms for these excitations could be found and that such solutions could be generated exploiting the topology of the system only if the network was charged and had surface spin half particles on it. Introducing surface spins adds a new topological feature to the surface: it has a spin structure. This means that there can be different ways of arranging surface spins in patterns that are topologically different. This means topologically distinct patterns cannot be deformed to each other. Thus if we intuitively think of surface spin as arrows on the surface an aligned linked array going round a tube of the network in the clockwise direction is topologically different from an array going round in the anticlockwise direction. Here we show how in the same surface network, the topological process that creates soliton pulse excitations also co- produce surface waveforms with EEG waveform like properties. A direct link between the topological charge carried by soliton excitations and the EEG like waveform it creates is established. There are no ad hoc features present in the scheme. All the results obtained follow from requiring that both input signals as well as the surface network's response to them respect the mathematical properties of surface introduced. We will identify the soliton excitations found as action potentials and the surface oscillations they co-produce as EEG waveforms.

The importance of topology for exploring global features of the brain is now beginning to be recognized in neuroscience and elsewhere. Topology is the mathematical discipline that studies spaces and structures that do not change under continuous deformations. For example a line and a circle are topologically different but a circle and a square or a triangle are the same. Topological structures are robust. They are global properties of a system. For this reason there is growing interest in using topological methods to identify hidden robust structures present in the vast amount of data available that describe the connectivity architecture of the brain's axon network. This is an important area of current research. Another area of exploration where topological and algebraic geometry methods are being used is to unravel the information contained in brain signals. A few representative references in these growing areas of research are: (Bassett,2020; Curto,2017; Reimann,2017; K.Hess, 2018; M.Marcolli,2019).

In the spirit of searching for global ways of understanding the functioning of the brain, we prove that, remarkably, it is possible to construct a special surface network that exactly captures the topological connectivity architecture of any hypothetical brain connectome and show (Sen,2021) that this surface network can generate action potential-like soliton excitations, by local input

signals represented by local surface deformations. The scheme proposed differs significantly from existing methods of signal generation, (Scott,2002; Heimburg,2005; Shrivastava,2020) in two important ways: signals are generated by global means where the topology of the surface network and the presence of surface spin half particles play an essential role and the soliton pulses generated carry with them the surface deformation information that create them. It was shown how the soliton signals can transfer this information to the pathways they traverse leaving a non-transient topologically stable helical magnetic structure: a memory substrate. The structure is produced by the alignment of surface spin half particles by their interaction with the transient helical magnetic field produced when charge carrying soliton signals move through the network. The structure is held together by spin-spin interactions and is stable due to its topological form. It is a periodic structure with a natural excitation frequency that was theoretically determined to be in the range $(1 - 30+)$ Hz (Sen,2021). This suggests that memories, stored in this way, may be retrieved by oscillating electromagnetic signals either external or internally generated that have frequencies that overlap with memory label frequencies. Memory retrieval is by a resonance excitation mechanism.

We now explain three important features of the scheme Sen(Sen,2021): the reason for choosing a special surface for the network, the reason for choosing special type of input signals and how the surface network produces one dimensional action potential-like voltage pulses are non linear soliton excitations that are solutions of a special non-linear differential equation called the non-linear Schroedinger equation.

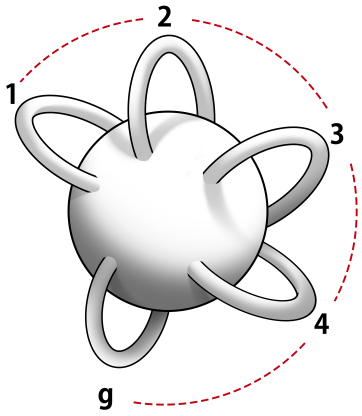

Fig. 1 Genus g surface

We can visualize a Riemann surface as a ubersurface covering the brain's assembly of three dimensional neurons. This is shown in Fig 3.

We first prove that it is possible to find a special mathematical surface network that exactly captures the topological architecture of any hypothetical

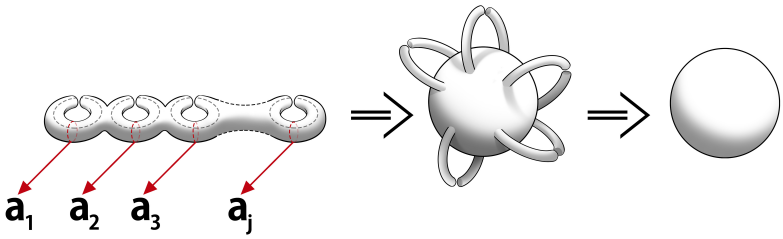

Fig. 2 Degenerate Riemann Surface with synapses

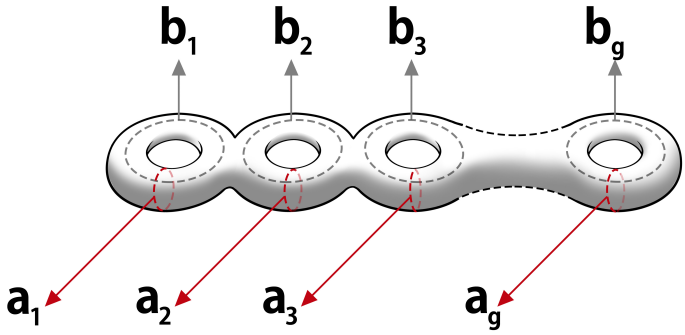

Fig. 3 Marked Riemann.

connectome of the brain even though the details of the hypothetical connectome connectivity architecture may not be known. Suppose we are given a hypothetical connectome of a specific brain. If this connectome is covered by a smooth surface then the theorem on the topological classification of surfaces, (Munkres,2014) tells us that no matter how complex and intricate are the unknown connection details of the underlying connectome the surrounding surface is topologically equivalent to an orderly array of donut surfaces. Thus the theorem tells us that (Fig 1, Fig 2A, Fig 3) all represent a Riemann surface. The unknown details of the connectome are reflected by one unknown number of the surface, namely, the number of donut surfaces required to represent it. We will call this mathematical surface an "ubersurface" as it can viewed as a mathematical surface that covers the brain's assembly of three dimensional individual linked neurons. If we suppose the ubersurface is smooth then it becomes a well studied mathematical surface known as a Riemann surface. We will explain what we mean by a smooth surface shortly. The number of donuts g present in the ubersurface is called the genus of the Riemann surface. The special $g = 0$ surface is a sphere and it can be related to a genus g by pinch deformations as shown in Fig 4.Thus a Riemann surface which looks

like a collection of thin tube like surfaces joined together in regions to form a compact overall structure exactly capture the topology of a given connectome.

There are, however, many possible smooth non-equivalent mathematical Riemann surfaces with spin structure that can capture the brain's intricate connectivity architecture. But within this class, it can be proved (Arbarrello,2001) that there is a special subclass that can generate the wide variety of brain-like signals by local surface deformations provided the special surfaces is charged and has a spin structure. A given spin structure is topologically stable and cannot be changed by smooth deformations.

The next step is to introduce input signals. An input signal on the surface will be taken to be a local set of surface deformations that are consistent with the mathematical features of the ubersurface. This is physically reasonable as our system is charged surfaces so that surface deformations will lead to local voltage changes. The response of the surface to these deformations is the signal. Surprisingly these are, as we will show, one dimensional multi-soliton solutions of the non-linear Schroedinger equation. Let us explain how such a precise result follows from the qualitative geometrical picture described.

To do this we need two mathematical results. The first result is that a charged Riemann surface with spin structure can also be described by an algebraic function called the Riemann theta function where all its variables are constructed from the topological coordinate variables of the Riemann surface (Sen,2021). The second is that the algebraic Riemann theta function describes a Riemann surface only if it satisfies a nonlinear identity called the Fay trisecant identity.(Mumford,1987)

Let us describe the topological variables used to describe a Riemann surface of genus g and then show how they are used to construct the variables of its associated Riemann theta function. In this paper no further details about Riemann surfaces or the Riemann theta function are required. The information about the variables is enough for us to explain the global method of signal generation described. Details of these mathematical objects are given in Mumford (Mumford,1987).

For a genus g Riemann surface the topological coordinates are, $2g$ loop coordinates $(a_i, b_i), i = 1, 2, ..g$ shown in Fig 3, that capture the topological connectivity properties of the Riemann surface and g smooth one forms $\omega_i(z)dz, i = 1, 2, ..g$, where z is a complex variable that represents a point on the Riemann surface. The set of one forms capture the smoothness of the Riemann surface. The one forms are normalized by requiring $\int_{a_i} du\omega_j(u) = \delta_{ij}$ where $\delta_{ij} = 0, i \neq j; = 1, i = j$, and the integral is a closed circuit along the loop coordinate a_i, surface spins are represented by spin fields $s_i(z), i = 1, 2$. The corresponding algebraic Riemann theta function has variables that are constructed from the topological coordinates of the Riemann surface. They are g complex variables $z_i, i = 1, 2, ..g$ constructed from one one complex variable z that represents a point on the Riemann surface by the map $z_i = \int_0^z du\omega_i(u), i = 1, 2, ..g$ and the symmetric complex valued matrix $\Omega_{ij} = \int b_j du\omega_i(u)$, where the integral is round a loop b_j, while the spins

$s_i(z), i = 1, 2$ on the Riemann surface are now represented by a set of $2g$ variables $(\alpha_i, \beta_i, i = 1, 2, ..g)$ called characteristics that can only take two values, namely $(0, \frac{1}{2})$ (Atiyah,1971,Mumford,1971). The charged nature of the Riemann surface makes the theta function a voltage function. The key requirement for the Riemann theta function to properly describe a Riemann surface is that it must satisfy a non-linear identity called the Fay trisecant identity.

We now have the concepts needed to explain how signals, generated by local pinch deformations, are soliton solutions of the non-linear Schroedinger differential equation. The idea is to use the Fay trisecant identity. Using the identity Mumford (Mumford,1987) showed that under pinch deformations the Fay identity becomes a non-linear differential equation so that the response of a Riemann surface to local pinch deformations described in terms of the Riemann theta function ,requires that the theta function must satisfy the non linear differential equation that now represents the Fay identity.

The underlying idea is a Principle of Compatibility that required all allowed Riemann surface local deformations to maintain the mathematical structure of the Riemann surface. Thus it is required that the local deformations introduced as input signals, deform the coordinate variables of the surface and can even change the nature the Riemann surface, should do so by following a path where at every step there is a Riemann surface structure present. At each step of the deformation the local topological coordinate variables of the Riemann surface change. This in turn lead to the deformation of the variables that define the associated Riemann theta function. For a special allowed deformations, called pinch deformations, where the circumference of tubes of the Riemann surface are reduced to zero as shown in Fig 4, the Fay non-linear identity becomes a one dimensional non-linear Schroedinger differential equation. Compatibility of the Riemann theta function with this deformed Riemann surface structure requires that it must be a solution of this non-linear differential equation. Thus solutions of non linear Schroedinger equations represent the response of the surface to pinch deformations. The emergence of the non-linear Schroedinger differential equation requires that the Riemann surface chosen belongs to a special class (Arberello, 2001). For this special class of Riemann surfaces local pinch deformations produce one dimensional action potential-like soliton voltage pulses. These voltage pulses carry charge and as they move through the network they generate a transient helical magnetic field that acts on the surface magnetic spin half particles assumed to be present and align them to form a non transient helical structure which is held in place by the spin-spin magnetic interactions and is topologically stable. The structure captures the nature of the transient magnetic field that created it which in turn reflects the nature of the moving action potential like signal. The structure is thus a memory substrate. The mathematical details are in Sen(Sen, 2021).

Here we take the next step and show that whenever a soliton excitation or any other non linear excitation is generated there are accompanying linear surface waveforms that are EEG waveform like and determine their expected

properties theoretically. With this step we will have a mathematical scheme for generating all observed brain electrical excitations.

The local surface deformations that generate one dimensional action potential like soliton pulse signals are pinch deformations of the Riemann surface, where the circumference of, say, k handles of a subunit of a Riemann surface of genus $g > k$ are reduced to zero (Fig 4), turning it into a spherical surface. Under such a deformation a train of k one dimensional solitons can be produced. These solutions were discussed in Sen(Sen,2021). The spherical surface created during signal generation is expected to be in an excited electrical state and have surface voltage oscillations. Our aim is to determine the properties of these oscillating waveforms. After the mathematical properties of these surface waveforms are established we will assume that the soliton pulses generated are brain action potentials and that surface oscillations are EEG waveforms and discuss the biological implications that follow from such an identification.

Results

We have briefly explain how surface waveforms are co-produced when pinch deformation generated excitations form in the surface network. Let us first link the surface waveform solutions on a spherical surface are directly related to the way they are created by soliton excitations. This step will directly relate properties of the EEG like waveforms to the soliton excitations that produce them. After that we we will proceed to discuss the nature and properties of these surface waveforms by solving the wave equation on the surface of a sphere.

Creating Surface waveforms

To link surface waveforms to solitons requires three mathematical ideas. The first is that k pinch deformations on a subunit of genus k required to produce a train of k solitons reduces the genus of the subunit to zero (Fig 4). The Riemann surface becomes a topological sphere. We can think of the spherical surface as a neuron and the input signals on it as coming from dendrites that are marked points on a sphere. This surface is charged and is expected to be in an excited state with surface voltage oscillations. This is a general result. The second is that surface oscillations on a spherical surface are solutions of a wave equation that is appropriate for a spherical surface and the third is that there are marked points on the spherical surface that correspond to pinch point where soliton effects enter. The soliton inputs at these points determine the nature of surface oscillations generated. We can think of these points as the location of primary dendrites on the soma.

A general wave equation has the structure,

$$\frac{1}{c^2}\frac{\partial^2\phi}{\partial t^2} - \nabla^2\phi = 0$$

where ∇^2 is the Laplacian operator. For oscillations on the surface of a sphere the Laplacian must have the symmetry of the sphere. This leads to the wave equation becoming a linear second order hypergeometric differential equation (Miller 2010) with three regular singular points (Yoshida,1987). We are interested in waveform solutions that fit together on a spherical surface without overlapping as these special waveforms will persist and should be observable. They tile the surface of the sphere. Thus step by step we are led to the conclusion that waveforms that tile the sphere are special and should be observed, if the global topological method of action potential like soliton generation is valid.

Soliton excitations carry a topological charge which we will shortly define. It is a topological phase. Remarkably these topological phases carried by soliton solutions completely determine the solutions of the hypergeometric equation. This is because solutions of the hypergeometric equation are uniquely determined by certain phases associated with its three regular singular points (Yoshida,1987). The set of phases form the monodromy group of the equation (Appendix A). We will show how the topological phases carried by solitons can fix the monodromy group phases. From this it follows that soliton input topological phases fix the nature of the waveforms on the sphere and furthermore these topological phases lead to tiling waveforms.

The monodromy group (Appendix A) associate phases to solutions. Specifically if a solution of the hypergeometric differential equation is transported round a singular point it is changed by a phase factor. The collection of phases at the three regular singular points of the hypergeometric differential equation form a group called the monodromy group. In our scheme the three regular singular points represent inputs from three dendrites to the cell body.

For more than three input to the cell body an appropriate generalized hypergeometric equation with more than three singular points is required. Solutions of this equation are also fixed by phases but the solutions are non tiling and are not uniquely determined by the input topological phases(Yoshida 1987). In this case knowledge of the ordering of the input phases is also required to uniquely determine a solution. Hence even though oscillations generated by more than three input phase signals may be present they do not form persistent patterns and hence will appear as a random background of oscillations. For this reason we do not consider them any further but focus on the case where only three soliton signals topological phases are involved. Since our mathematical results are intended to represent events on the surface of neurons we note that there is biological support for considering three input pinch deformations since the number of primary dendrites on a soma, that represent input signals to neurons, is between five and seven with a median value of between three and four(Oga 2016,Dharani 2015).

Surface waveform creation by Pinch Deformation Signals

Let us now give relevant details. All pinch generated signals carry the pinch deformation parameter information that create them but they also carry a

topological phase. This phase is fixed by the discrete characteristic labels $(\alpha_i, \beta_i, i = 1, 2, ..g)$ of the Riemann theta function (Sen,2021) that describes the signal, where each $\alpha_,\beta_i$ can only take one of two values, namely $0, \frac{1}{2}$. Thus each signal has a topological twist phase factor W where $e^{4i\pi \sum_{i=1}^{g} \alpha_y \beta_i} = e^{iW}$.

We next explicitly relate the soliton signal phase twists $W_i, i = 1, 2, 3$ at three points to monodromy group phases. It is known that solutions that have a finite monodromy group are tile the sphere and show that this condition holds for the monodromy group generated by soliton topological phases. The tiling solutions belong to 5 frequency classes (Yoshida,1987) that we identify as our oscillatory stable waveforms. These solutions will persist and should be observable. They reflect the five Platonic solids of antiquity.

Let us proceed to fix monodromy phases from soliton phases. We assume that a unit twist associated with a soliton excitation at a pinch deformation point produces a twist of, e^{it} at a regular singular point of the hypergeometric differential equation on Σ_0, the topological sphere created. Then a topological twist W produces a twist $(e^{it})^W = e^{itW}$. This twist is, as we discuss in Appendix A, related to the difference between the characteristic exponents of solutions of the hypergeoemtric equation at that point.

We now recall that a soliton solution has a topological twist phase factor given by the integer $W = 4 \sum_{i=1}^{g} \alpha_i \beta_i$, where (α_i, β_i) are the characteristics of the Riemann theta function. A characteristic is said to be an even/odd characteristics depending on whether $e^{i\pi W} = \pm 1$. For solitons to be produced the Riemann theta function must have odd characteristic. We can now fix the allowed range of values t can take by using a compatibility condition which i requires that the singular point twist e^{itW} matches topological twist factor $e^{i\pi W}$ of the soliton. But this factor can must be -1. Thus we have the matching condition $e^{itW} = -1$ This fixes the allowed values of t. Possible values of t are $\frac{\pi}{2}, \frac{\pi}{3}, \frac{\pi}{4}, \frac{\pi}{5}$ corresponding to $W = 2, 3, 4, 5$. We will see in the next section that these values agree with those of the explicit tiling solutions on the surface of a sphere found by Schwarz (Schwarz,1873)

Identifying Special Solutions of the Hypergeometric equation

We now describe explicit tiling soltions of the hypergeometric equation on a sphere studied by Schwarz,(Schwarz,1873). Later we will consider a subclass of Schwarz solutions that have simpler solutions with oscillation frequencies given by a simple formula. This subclass is important as they form a complete set of basis functions on a spherical surface.

Schwarz List of solutions

Schwarz (Schwarz,1873) found 15 algebraic solutions tiling solutions of the second order linear hypergeometric differential equation on the surface of a sphere. Let us give an intuitive reason for this remarkable result. Three facts are helpful.

The first is a property of spherical triangles drawn on the surface of a sphere of radius R with sides that are great circles. Euclid's result that the sum of the angles α, β, γ of a triangle on a plane add up to π radians is now replaced by the result that the sum of angles of a spherical triangle is related to its area in the following way (Wolfram):

$$\alpha + \beta + \gamma - \pi = \frac{A}{R^2}$$

where A is the area of the spherical triangle. Thus the sum of the angles fixes the area of a spherical triangle for a given radius R. Hence given that a sphere of radius R has area $4\pi R^2$ we can find the allowed identical set of triangle that can tile the sphere. This leads to five cases discovered by Plato: the five Platonic solids whose surfaces suitable mapped on to the surface of a sphere tile it using identical subunits.

The second fact is that the Laplacian operator necessary to study waves on must have the symmetry of a sphere. This requirement leads to the second order hypergeometric differential equation (Miller 2010).

The third fact is that the second order hypergeometric differential equation has two linearly independent solutions with three regular singular points and that these two independent solutions are completely determined by the way they change as they are transported round singular points (Yoshida,1987)(Appendix A). Such a transport produces a phase change of the solution called its monodromy, which is a phase angle. The presence of three regular singular points leads to three angles. These angles, if they have the right set of values, can be represented as the angles of a spherical triangle. If these triangles have appropriate angle values they can tile the sphere. This means that these waveforms cover the surface of the sphere without overlapping and thus persist stably. For this to happen the solutions have to have special values for their monodromy phases.

When this happens we have stable surface waveform bands. The sides of the triangles are the nodes of the waveforms. A mathematical description of the way tiling of spheres and special solutions of the hypergeometric equation are related is outlined in Appendix B.

A list of such solutions is available (Vidunas 2008,2009). Examples of tilings are shown in fig 5: Schwarz Triangles

Surface waveform Frequency Estimates

We can give a simple geometric argument to estimate the frequencies of tiling solutions. Later we will determine the explicit analytic form for tiling waveforms and find a formula for their frequencies directly by solving the wave equation on a sphere.

The wave like nature of tiling solutions comes from from the fact that they have a periodicity that is induced by the tiling. A solution in one tiling sector has to smoothly join onto the solution in the next sector. This periodicity

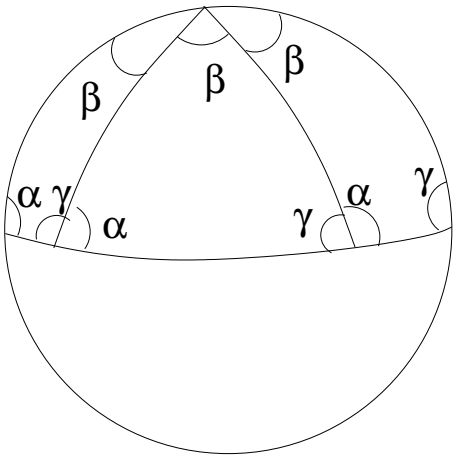

Fig. 4 Schwarz Tiling.

generates a two dimensional waveform. The size of these two dimensional excitations can be estimated by the area of a tiling segment. If we take the speed of these waves to be approximately tiling independent then we can estimate the frequency of the different waves as being proportional to the inverse of their size.

Let us carry out this frequency estimate for 5 algebraic solutions of Schwarz and then compare our frequency estimates with observed EEG frequencies. The favorable agreement is noted but we continue to treat these results as mathematical results of our surface network The tilings are described by three angle labels a, b, c that fix the tiling area A, for a spherical triangle, is fixed by by angles of the triangle by the simple formula $\frac{A}{r^2} = a+b+c-\pi$, where r is the radius of the sphere. We tabulate the tiling areas, estimated wave frequencies and state the associated Platonic solid:

Solid	**Area**	**Schwarz labels**
Dihedral	$\frac{p}{n}$	$(\frac{1}{2}, \frac{1}{2}, \frac{p}{n} \leq \frac{1}{2})$
Tetra	$\frac{1}{6}$	$(\frac{1}{2}, \frac{1}{3}, \frac{1}{3})$
Tetra	$\frac{1}{3}$	$(\frac{2}{3}, \frac{1}{3}, \frac{1}{3})$
Cube	$\frac{1}{12}$	$(\frac{1}{2}, \frac{1}{3}, \frac{1}{4})$
Icosa	$\frac{1}{30}$	$(\frac{1}{2}, \frac{1}{3}, \frac{1}{5})$
Icosa	$\frac{1}{15}$	$(\frac{2}{3}, \frac{1}{5}, \frac{1}{5})$

The areas are in units of π. The Schwarz labels are the angles a, b, c written as $a = \frac{\pi}{p}, b = \frac{\pi}{q}, c = \frac{\pi}{s}$. The frequencies are proportional to the inverse of the areas listed. We set the basic frequency equal to one Hertz. We then have the frequency estimates,

Solid	Size	Frequency	EEG	Predicted	Observed
Dihedral	$\frac{p}{n}$	≥ 2	All waves	$\frac{1}{n}A$	All waves
Tetra	$\frac{1}{3}$	3	delta (.5-3)	$200\mu V$	$200\mu V$
Tetra	$\frac{1}{6}$	6	theta(3-8)	$100\mu V$	$50\mu V$
Cube	$\frac{1}{12}$	12	alpha(8-12)	$50\mu V$	$50\mu V$
Dodaca	$\frac{1}{15}$	15	beta(12-30)	$40\mu V$	$< 50\mu V$
Icosa	$\frac{1}{30}$	30	gamma(30–42)	$20\mu V$	$10\mu V$

We compare our mathematical results with the observed 5 types of global EEG brain wave frequencies, namely, the delta (.5-3 Hz), theta (3-8 Hz), alpha (8-12 Hz), beta (12-30 Hz), and gamma (30-42 Hz) are listed (Liu 2013). The predicted frequency values setting the base frequency to one hertz are listed. Thus our estimates roughly agree with observations. This encouraging result is a first step in our identifying the surface network signals as brain signals and the surface oscillations that we are studying as EEG waveforms. For the moment we continue to carry out our mathematical analysis and regard the comparison result as an interesting coincidence. To get the frequencies a base frequency of one Hertz was chosen and the sphere radius r was set to one. For arbitrary r the frequencies scale by the factor $\frac{1}{r^2}, r > 0$. However we have set the basic frequency to be one hertz. This fixes the scale. Thus setting $r = 1$ is justified. It is not an extra parameter of the model. The amplitudes numbers predicted use an input value of $200\mu V$ for delta waves.

We also note that since the Schwarz solutions are solutions of a linear system a general surface waveform will be a linear superposition of the fundamental set of eigensolutions of the system.

Surface Waveforms: Fractional Legendre functions

We next determine analytic expressions for waveforms and find an explicit formula for their allowed frequencies of tiling solutions from the mathematical fact that the associated Legendre functions of fractional order, $P_\nu^\mu(z)$, form a complete set of basis functions and that they are sphere tiling solutions that can be used to represent dihedral, tetrahedral, and cubic symmetry classes (Maier 2018). These solutions are also solutions of a wave equation on a sphere. Using these facts we wil determine the oscillation frequencies of the waveforms. Finally since these special tiling solutions form a basis set of functions they can be used to represent any arbitrary square integrable function $f(z)$ on the sphere. Thus, any such function $f(z)$, can be written as,

$$f(z) = \sum_{n=-\infty}^{i=+\infty} c_n P_{\nu_0+2n}^{\mu}(z)$$

where the points z represent arcs on the sphere. From this result and the orthogonality property,

$$\int_{z=-1}^{z=+1} P_{\nu_1}^{\mu}(z) P_{\nu_2}^{-\mu}(-z) = \alpha(\mu, \nu_1)\delta_{\nu_1,\nu_2}$$

we obtain the completeness result,

$$\delta(z - z') = \sum_{n=-\infty}^{n=+\infty} \frac{P_{\nu+2n}^{\mu}(z) P_{\nu+2n}^{-\mu}(-z')}{\alpha(\mu, \nu + 2n)}$$

The dihedral tiling class corresponds to setting $\mu = \frac{1}{2}, \nu = -\frac{1}{2}$. We also have the completeness result,

$$\delta(t - t') = \int d\omega e^{i\omega(t-t')}$$

A more general class of basis functions can also be used for representing functions defined on the sphere rather than along arcs on the sphere. They are the analog of the usual spherical harmonics. We display the ones related to dihedral tiling. We have

$$Y_{-\frac{1}{2}+2n}^{-\frac{1}{2}}(\theta, \phi) = N_{(\frac{1}{2}, 2n-\frac{1}{2})} e^{-i\frac{\phi}{2}} \sqrt{\frac{8}{\pi \sin\theta}} \cos(2n - \frac{1}{2})\theta)$$

where $n = 1, 2, ..$ and $N_{(-\frac{1}{2}, 2n-\frac{1}{2})}$ is a normalization factor. It is evaluated in the next section. Using this function we can plot EEG waveform-s in two dimensions and display their tiling property.

The completeness property of these solutions and the fact that they are related to solutions of the wave equation on a sphere will now be used to construct a Greens function(Morse, 1953) appropriate for studying time dependent modulations of our surface waveforms.

Construction of Greens function for surface wave modulations

The Greens function captures essential symmetry features of tiling waveforms and thus can be used to study their responses to external or internal signals. It satisfies the equation,

$$(\frac{1}{c^2}\frac{\partial^2}{\partial t^2} - \nabla^2) G(z, t : z', t') = \delta(t - t')\delta(z - z')$$

We replace the right hand side with the delta function representations chosen, with $\mu = \frac{1}{2}, \nu = -\frac{1}{2}$, if we use the dihedral tiling waveforms, with the ∇^2 operator with the symmetry of the sphere and suppose that the Greens function

depends only on $(t-t')$, and $0 \leq t' \leq t$. Then

$$G(z,z',t-t') = \sum_n \int d\omega \frac{P^{\mu}_{\nu+2n}(z)P^{-\mu}_{\nu+2n}(-z')}{(-(\frac{\omega^2}{c^2}) + \omega_n^2)} \frac{e^{-i(t-t')\omega}}{\alpha(\mu,\nu+2n)}$$

where $\nabla^2 P^{\mu}_{\nu+2n}(z) = -\omega_n^2 P^{\mu}_{\nu+2n}(z)$. carrying out the ω integral we get

$$G(z,z',t-t') = i\pi \sum_n (\frac{e^{-i\omega_n(t-t')}}{\omega_n}) \ \frac{P^{\mu}_{\nu+2n}(z)P^{-\mu}_{\nu+2n}(-z')}{\alpha(\mu,\nu+2n)}$$

The modulation $m(z,t)$ of an surface waveform due to an input signal $s(t,z)$ can now be calculated. We have

$$m(z,t) = \int dt' \int dz' G(z,t,z',t')s(z',t')$$

We now note that the set of dihedral tiling solutions, on their own, also form a complete set of basis eigensolutions, and hence can be used to represent all allowed tiling surface waveforms. Hence we will just use these waveforms in our discussions. These dihedral tiling waveforms, labeled by an index n have frequencies

$$\omega_n = \sqrt{n^2 - \frac{1}{4}}, \quad n = 2, ..$$

and their waveform shapes are given by the fractional spherical harmonics,

$$Y^{-\frac{1}{2}}_{n-\frac{1}{2}}(\theta,\phi) = N_{(-\frac{1}{2},n-\frac{1}{2})} \ e^{-i\frac{\phi}{2}} \sqrt{\frac{8}{\pi \sin\theta}} \ \cos(n-\frac{1}{2})\theta$$

where $n = 1, 2, ..$. Thus we have found explicit expressions for surface waveforms and a formula for their allowed frequencies.

The general class of algebraic Schwarz solutions have been thoroughly studied by Vidunas (Vidunas 2008, 2009). Here, for reasons given, we restrict ourselves to the less general dihedral as they have simple mathematical properties and at the same time form a complete basis set of functions. We can now relate the frequencies of these waveforms to their amplitude by calculating the normalization factor $N_{(-\frac{1}{2},2n-\frac{1}{2})}$. This will determine the way it scales with n and thus establish a relationship between the amplitude and the frequency of a waveform. Using the normalizations of Maier(Maier 2018) for $P^{\mu}_{\nu}(\theta), P^{-\mu}_{\nu}(\theta)$ that can be related their norm $P = P^2 = \int_{\pi}^{+\pi} d\theta \sin\theta P^{\mu}_{\nu}(\theta)P^{-\mu}_{\nu}(\theta)$ can be evaluated. Writing $P^{\mu}_{\nu}(\theta) \to P\frac{P^{\mu}_{\nu}(\theta)}{P}$, with $(\mu = \frac{1}{2}, \nu = 2n - \frac{1}{2})$ the n dependence of the amplitude is fixed by P which is,

$$P = \sqrt{\sqrt{\frac{2}{\pi}} \ \frac{\Gamma(\frac{3}{4})}{\Gamma(\frac{5}{4})} \ \frac{(4n+2)}{(2n+\frac{1}{2})(2n+\frac{3}{4})}}$$

Thus a clear inverse relationship between the amplitudes and frequencies is established. Since the dihedral tilings can be used to represent all other tiling solutions, this relationship is valid for all surface waveforms.

There are corresponding set of basis functions for some other tiling waveforms. For, example, for a tetrahedral or octahedral tiling generated surface waveforms, the frequencies are of the form,

$$\omega = \sqrt{(\nu + \frac{1}{2} + 2n)(\nu + \frac{3}{2} + 2n)}$$

with appropriate fixed values for (ν, μ) and (n, m) integers $(0, 1, 2, ..)$ that reflect the symmetry of the tiling, there is a corresponding waveform $Y^{\mu+m}_{\nu+\frac{1}{2}+2n}(\theta, \phi)$. These expressions may be directly used also show the inverse relationship between waveform amplitudes and their frequencies. Thus, for the octahedral tiling case an explicit expression for waveforms is available (Maier 2018). We have,

$$P^{\frac{1}{4}+m}_{-\frac{1}{6}+n}(\cos\theta) \;=\; 2^{-2m-3n}\;\Gamma(\frac{3}{4}-m)^{-1}\;(\sin\theta)^{-\frac{1}{4}-m}B_{+}^{\frac{1}{4}+3m+3n}r_n^m(\frac{B_-}{B_+})$$

$$B_\pm \;=\; \cos(\frac{\theta}{3}) \pm \sqrt{\frac{4\cos^2(\frac{\theta}{3})-1}{3}}$$

where $r_n^m(\frac{B_-}{B_+})$, for $(n, m) \geq 0$ are Heun polynomials (Ronveaux 1995) of degree $(3n+2m)$ with octahedral symmetry. However we will not consider these cases any further and in all our subsequent work and discussions we will always use the dihedral waveforms to approximate all other tiling solutions and thus represent all surface waveforms.

At this stage we have established mathematical tools to study the response of the surface waveforms to external signals, we have found their oscillation frequencies and their explicit form. We now take the next step and assume that the soliton excitations of our network represent brain signals and our surface oscillations co-produced with any signal created by pinch deformations as EEG waveforms. We thus identify mult–soliton solutions with spike trains, dark soliton solutions that are oscillations on top of a high energy background, with bursts and transient localized excitations that can be generated by pinch deformations, with blocking signals that prevent certain certain brain circuits from functioning, as observed during sleep. We can then apply the techniques established to analyze observed EEG events. We carry out such an analysis to discuss the observed sequence of brain EEG events during NREM sleep,namely, K-complexes-Sleep-Spindles and Sharp -Wave Ripples.

Modeling K-complexes-Sleep-Spindles-Sharp Wave Ripples

In NREM sleep delta waves are observed and at intervals of 1-1.7 minutes large sharp spikes, K-complexes, are observed that have amplitudes in excess

of 100 mV in the background high amplitude of slow waves and delta waves (1.6-4.0) Hz present. These excitations have duration in excess of 500 ms and are followed by spindle shape oscillations of duration a few seconds of frequency in the range $10-15$) Hz, followed by sharp wave ripples (De Gannaro 2003,Ioannides 2019). These EEG events happen in this order.

We interpret this sequence of events as a mechanism of memory consolidation and the transference of memory copies from one region of the brain, possibly the hippocampus, to another region of the brain, possibly the frontal cortex (Buzsaki 1989, 2015). The first step in the sequence of events described is assumed to be due to a major transient localized cortical that prevents regions of the brain from receiving or processing information for the period of time. It is a local blocking event. The triggering event should have high voltage, be transient, and localized to an appropriate brain region with a duration in excess of 500 ms. During this period of time other signals cannot proceed in the region where the event has occurred: the region is thus isolated from other signals. Such a blocking transient event, we suggest is responsible for the K-complex modulation of the delta wave that is co-produced with it. A mathematical example of such a transient cortical events which are created by pinch deformation input signals, exists. Examples are rational breather and peakon solutions(Kalla 2011).

We next suggest that sleep spindles observed reflect the modulation of delta waveforms by the frequency label of memory information encoded (Sen et al 2021, submitted) in topologically stable helical magnetic traces. It was shown that they have a frequency label in the range $(2-30+)$ Hz (Sen 2021).

Finally the memory trace modulation on the high voltage delta waves. interact with underlying neurons to produce, by a resonance process, memory copy carrying burst excitations which in turn modulate the delta waveforms co-produced and show up as sharp wave ripples in the EEG signals. The produced bursts are interpreted as copying and transferring memory information. Because of the extensive nature of the blocking signal the visual and auditory sensory pathways do not respond to these activities.

In earlier work (Sen et al. 2021) it was shown that memories may be stored non-locally as closed helical magnetic traces $\Delta\vec{B}(x)$ in the pathways traversed by multi-soliton excitations. The non transient trace has a natural excitation frequency in the oscillation frequency range $(1-30+)$ Hz. We now calculate the modulation of a delta waveform potential as it moves over such a magnetic memory trace. In an earlier section we showed that the delta waveform potential was $V(\theta,\phi,t) = Ne^{-i\frac{\phi}{2}}\sqrt{\frac{8}{\pi\sin\theta}}\ \cos(2n-\frac{1}{2})\theta\ e^{i\omega_0 t}$,in terms of spherical polar coordinates, with $\frac{pi}{2} < \theta < \pi$, where N was a normalization constant and $\omega_0 = \sqrt{n^2-\frac{1}{4}}, n = 2$. Using this expression we can calculate its the gradient $-\nabla V$ which is an electric field that acts on charges e on the tube causing them to move. For a qualitative understanding of this effect, which we show these effects produces spindles, we replace the (θ,ϕ) dependence of $V(\theta,\phi,t)$ by a simpler expression but we retain its theoretically motivated time dependence.

Thus we set $V = V_0 \sin\theta \sin\phi \cos t$ for the delta waveform, so that $\omega_1 \approx n$. Then $V = V_0 y \cos t$ in Cartesian coordinates and we have,

$$\begin{aligned} E_y &= -\nabla_y V = V_0 \cos t \\ m\frac{dv_y}{dt} &= eE_y \\ v_y(t) &= \frac{V_0 e}{m} \sin t \end{aligned}$$

This moving charge interacts with the helical magnetic trace present and excites it to its natural frequency $\omega_0 = \frac{2\pi v_0^2}{cr_s}$ found in Sen(Sen,2021), where v_0 is the charged soliton pulse speed that led to the magnetic memory trace. Thus we have the excited magnetic field given by,

$$\vec{B}(t, \vec{x}, r_s) = B(\vec{x})(\cos(\frac{2\pi v_0^2 t}{cr_s}), r_s \sin(\frac{2\pi v_0^2 t}{r_s}), z = v_0 t),$$

where r_s is the radius of the tube, c the velocity of light in the medium.Thus the natural excitation frequency of the structure is $\omega_0 = \frac{2\pi v_0^2}{cr_s s}$. To calculate the modulation of the EEG wave we use the fact that the moving charge interacts with this magnetic field via a Lorentz force (Jackson 1999). Thus if the charge is moving with velocity v_y it interacts with the x component of the magnetic trace, it produces a force in the z direction and hence generates a force F_z from which modulating potential ΔV can be determined by noting that $F_z dz = -\Delta V$. The force is given by

$$F_z = \frac{e}{c} B v_y(t) \cos\omega_0 t$$

and the modulating potential is $\Delta V = -F_z dz$. Thus we find that ΔV is,

$$\Delta V = \frac{e^2 V_0}{mc} B(\sin z) \sin(\omega_0 z) dz, \ 0 \leq z \leq L$$

where we have used z to parametrize time, setting $B_z = z = v_0 t$ for the helical magnetic memory trace, and we have set $v_0 = 1$. This is a spindle. It carries the helical magnetic memory trace excitation frequency.

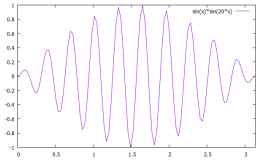

Fig. 5 Sleep Spindle

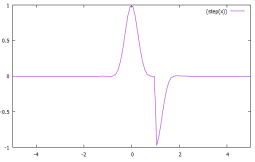

Fig. 6 K Complex

Thus ΔV, provides a copy of the memory traces. We now interpret our results in terms of brain excitations. The modulation theoretically determined has the shape of a sleep spindle, as $\omega_0 >> 1$. From observations we find that $\omega_0 \approx 10 - 15$ Hz which is consistent with our earlier theoretical result (Sen,2021) that memories are stored non-locally as topologically stable helical magnetic traces with a theoretically determined frequency in the range $(1-30+)$ Hz. The result obtained will remain valid even if we had used our theoretically determined expression for the delta waveform potential rather than our simple representation of it. The difference would be in, not in the qualitative shape of the sleep spindle but in its detailed nature as there would now be a spatial dependence present in $\vec{v}(t)$ with the combination $(v_y B_x - v_x B_y)$ rather than just the term $v_y B_x$ that we used.

Transient Signals and K-complex

We now give the mathematical details that show how the suggestion that a high energy blocking signal, which is a transient solutions of the non-linear Schroedinger equation can explain a K-complex modulation. Explicit mathematical examples of such transient solutions exist, such as the peakon solution and rational breather solution and their analytic forms are available (Kalla 2011) but, we simplify our analysis by approximating the known analytic solutions for transient excitations, using the following simple expression,

$$\psi(\theta,\phi,t) = \delta(\theta-\theta_0)\delta(\phi-\phi_0)e^{-(\omega_n t)^2}\Theta(t) - \Theta(t-\frac{1}{\alpha})\delta(\theta-\theta_1)\delta(\phi-\phi_1)$$

where $(\theta_1 = \theta_0 + \Delta, \phi_1 = \phi_0 + \Delta)$, and $\Theta(t) = 1, t > 0$ and is zero otherwise, the Heaviside Theta function. The Greens function, for surface dihedral waveforms is given by,

$$G(z,z',t-t') = i\pi(\frac{e^{-i\omega_n(t-t')}}{\omega_n})\ P^{\frac{1}{2}}_{-\frac{1}{2}+2n}(z)P^{-\frac{1}{2}}_{-\frac{1}{2}+2n}(-z')$$

$$P^{-\frac{1}{2}}_{2n-\frac{1}{2}}(\theta) = \sqrt{\frac{8}{\pi\sin\theta}}\ \cos(2n-\frac{1}{2})\theta),$$

For our qualitative discussion we drop normalization factors and ignore the spatial oscillations of the waveforms. Then any surface waveform modulation

due to a transient localized excitation, can be plotted using,

$$\begin{aligned} M(t) &= M_1 + M_2 \\ M_1 &= A\frac{1}{\sqrt{n}}e^{-(\omega_n t)^2}\cos\omega_n t, \quad -T < t < +T \\ M_2 &= A\frac{1}{\sqrt{n}} - e^{-(\omega_n (t-2T))^2}\cos\omega_n t, \quad +T < t < +3T \end{aligned}$$

with $\omega_n = \sqrt{4n^2 - \frac{1}{4}}$. For numerical work an appropriate gluing function M_{12} is required. The value of the constant A, has to be chosen.

Thus a K-complex modulation of a EEG delta waveform can be understood as a modulation of the delta waveform by a high energy transient blocking excitation. The transient event is required to have high energy, as the delta waveform co-produced with it and then modulated by it, has high energy. But such transient excitations can theoretically exist with lower energies, ranges and duration. We sketch the possible energies, ranges and durations, that such excitations can have, using brain EEG waveform information. We then suggest that all of these transient excitations should be observed and that they all play a role in the functioning of the brain.

Prediction of Range, Energy and Duration of Blocking Signals

We can predict the duration, range and energies of any one of these theoretically allowed transient excitation that produces K-complex like EEG modulation by linking these parameters to the EEG waveforms that they modulate. Our estimate for duration is, thus, $\tau_n \approx \frac{1}{\omega_n}$, for energy $\approx V$, the voltage amplitude of the waveform, with a range given by the area fraction of a sphere tiled by the waveform. Hence for a delta wave these estimates suggest a duration $\tau_1 \approx \frac{1}{2}$ seconds which is ≈ 500 ms (Weigenand 2014). We tabulate the results, listing the n value of an EEG waveform, and the amplitude, in mV, and duration,in ms, of K-complexes EEG modulations created by transient localized excitations.

Waveform	Wave Number	Amplitude	Duration	Range
Delta	1	100	500	$\frac{\pi}{2}$
Theta	3	30	100	$\frac{\pi}{3}$
Alpha	6	16	50	$\frac{\pi}{6}$
Beta	10	10	30	$\frac{\pi}{10}$
Gamma	50	2	6	$\frac{\pi}{50}$

We speculated earlier that a person can perhaps initiate transient localized blocking events by chemical means. Perhaps the local release of dopamine and nitric oxide signals (Kali 2010) play such a role in the case of K-complexes. This is because dopamine has been identified as a system manager for cortical activity (Hong 2013) while nitric oxide has been identified as playing a key role in sleep (Kalinchuk 2010). If this is true then blocking dopamine and nitric

oxide signals would stop K-complexes and thus prevent the method of memory consolidation and transfer suggested.

Another implication of this speculation is that those that have a greatly reduced number of K-complexes during NREM should not be able to store long term memories. This speculation can be tested.

Plotting EEG waveforms in the dihedral approximation

A representative plot for a Delta waveform is plotted.

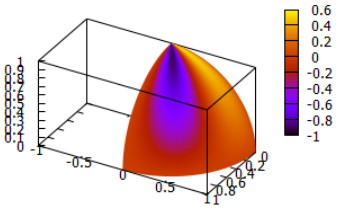

Fig. 7 EEG Delta Wave

We next plot a sample of predicted two dimensional waveform shapes for a class of EEG waveforms, tabulate their predicted frequencies and amplitudes and compared them with observations. These plots clearly show the tiling nature of the waveforms. Observed EEG waveforms are expected to be linear combinations of these waveforms with certain waveforms dominating depending on circumstances.

Our first step is to show that the solutions constructed are indeed tiling solutions, which means that they must vanish on the sides of an appropriate spherical triangle on the surface of a sphere. We select the following set,

$$Y^{-\frac{1}{2}}_{2n-\frac{1}{2}}(\theta,\phi) = N_{(-\frac{1}{2},2n-\frac{1}{2})}\ e^{-i\frac{\phi}{2}}\sqrt{\frac{8}{\pi\sin\theta}}\ \cos(2n-\frac{1}{2})\theta$$

where $n = 1, 2, ..$. The angles (θ, ϕ) are spherical polar coordinate angles with ranges $(0 \leq \theta \leq \pi, -\pi \leq \phi \leq +\pi)$. To construct tiling solutions that vanish on the sides of a spherical triangle the following variable changes are required$\theta \rightarrow \theta' = \frac{\theta}{2}, \phi \rightarrow \phi' = \frac{\phi}{2n}$ and we require that the solution be periodic

in ϕ'. In terms of these variables, the solution becomes,

$$S^{-\frac{1}{2}}_{2n-\frac{1}{2}}(\theta', \phi') = \frac{1}{\sqrt{n}} \cos(n\phi') \sqrt{\frac{1}{\sin 2\theta'}} \cos(2n - \frac{1}{2})2\theta'$$

where the range of the angles are now $(0 \leq \theta' \leq \frac{\pi}{2}, -\frac{\pi}{2n} \leq \phi \leq +frac\pi 2n)$. We check that this solution vanishes when $\theta' = \frac{\pi}{2}$ and when $\phi' = \pm\frac{\pi}{2n}$ which define the three sides of a spherical triangle. Thus we have constructed a tiling solution. To plot this waveform the expression obtained should be multipliede by $\sin(2\theta')$. We have included a normalization factor $\frac{1}{\sqrt{n}}$ which is an approximation of P defined by $P^2 = \int_{\pi}^{+\pi} d\theta \sin\theta P^{\mu}_{\nu}(\theta) P^{-\mu}_{\nu}(\theta)$ with $(\mu = \frac{1}{2}, \nu = 2n - \frac{1}{2})$ the n dependence of the amplitude is fixed by P[27] which is,

$$P = \sqrt{\sqrt{\frac{2}{\pi}} \frac{\Gamma(\frac{3}{4})}{\Gamma(\frac{5}{4})} \frac{(4n+2)}{(2n+\frac{1}{2})(2n+\frac{3}{4})}} \approx \frac{1}{\sqrt{n}}$$

It is now clear that the amplitudes are inversely related to frequencies and we list, in tabular form, the frequency and amplitude predictions made for EEG waveforms in this approximation .

Solid	**Size**	**Frequency**	**EEG**	**Predicted**	**Observed**
Dihedral	$\frac{p}{n}$	≥ 2	All waves	$\frac{1}{\sqrt{n}}A$	All waves
Dihed	$\frac{2}{2}$	1	delta (.5-3)	$200\mu V$	$200\mu V$
Tetra	$\frac{1}{6}$	6	theta(3-8)	$80\mu V$	$50\mu V$
Cube	$\frac{1}{12}$	12	alpha(8-12)	$57\mu V$	$50\mu V$
Dodaca	$\frac{1}{15}$	15	beta(12-30)	$40\mu V$	$< 50\mu V$
Icosa	$\frac{1}{30}$	30	gamma(30–42)	$28\mu V$	$10\mu V$

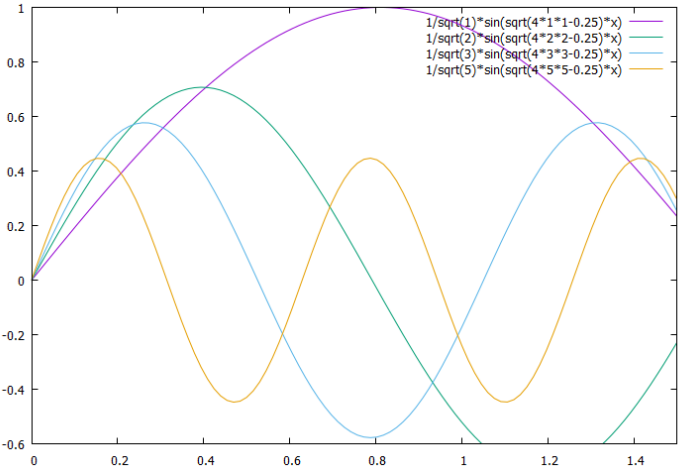

Fig. 8 Frequency-Amplitude Plots

Discussion

The central idea of this paper is that it is possible to generate all observed brain excitations by exploiting the topological features of the brain's connectivity architecture in a surface network that we prove exactly captures the topological connectivity of a hypothetical unknown brain connectome. if this surface network is charged and has surface spin half particles then we showed in an earlier paper, that by exploiting the global topological features of the network, a wide variety of one dimensional soliton pulse signals, with action potential like features can be generated, by local pinch deformations (Sen,2021). Furthermore these pulse signals were shown to carry input information that created them and can transfer and store this information as a memory substrate in the form of a surface helical spin structures. The memory structure is an alignment of surface spins, it is topologically stable and has a natural excitation frequency that is theoretically estimated. Memory storage is magnetic and is in the pathways between engram cells. The presence of spin half surface particles is essential.

Here we have shown that the same surface network can also produces EEG waveform like surface oscillations whenever non linear action potential like solitons are generated by local pinch deformations. The explicit form and frequency bands, of EEG waveforms, of these surface oscillations are theoretically determined and a precise relationship between a soliton excitation and the EEG waveform it co-produces is found. The analytic form of the surface oscillation and their frequencies is determined. It is found that these frequency must belong to five discrete classes that correspond to the Platonic tiling of a spherical surface, and that there is an inverse correlation between the frequency of a waveform and its amplitude. These theoretical predictions are consistent with observations. A further general prediction of the scheme is that EEG waveforms have a universal nature, that is, they should have the same structural properties for all creatures that have neurons and synapses(Bullough,2002, Fingelkurts 2014).

The non linear excitations were shown (Sen,2021) to be one dimensional soliton pulse solutions of the non linear Schroedinger equation, while the co-produced surface oscillations are linear waveforms, that are solutions of the linear hypergeometric differential equation on the surface of a sphere.

We will assume that the soliton pulses represent brain signals(Shrivastava,2012, Mussell,2020) and the surface oscillations, co-produced, are EEG waveforms, then all the mathematical properties of the surface oscillations and soliton signals derived theoretically became predictions. The method of EEG waveform generation proposed is unconventional. (Nunez 2006a,2006b, DaSilva, 1991, 2010,Jones,2016,Klimeschi,2018) but, as we suggest, it places EEG waveforms as an essential excitation for the cognitive functioning of the brain.

The suggestion that EEG waveforms play an essential role in the functioning of the brain is based on the mathematical results obtained. Thus in our

discussion of the K-complex initiated sequence of EEG events, observed during non rapid eye movement (NREM) sleep, it is suggested that the sequence of EEG events observed can be explained by a sequence of brain excitations where each step of the sequence has a mathematical correlative. The start of the sequence is by a high energy transient pinch generated excitation that blocks other signals from accessing certain brain circuits. Such transient excitations can be represented in the scheme as a rational breather or peakon solutions of the non linear Schroedinger equation and can be produced by suitable pinch deformations(Kalla,2012). A high energy transient blocking signal will co-produces a high energy EEG delta waveforms as we saw. The delta waveform is then modulated by the transient signal to produce the K-complex shape. The hypothesis that blocking signals can co-produce EEG waveforms is supported by observations(Becker 1985). The subsequent sequence of events that follow a K-complex excitations were interpreted as the modulation of a delta waveform by the helical frequency of a memory trace labeled (Sen, 2021) to produce a sleep spindle which, in view of its high energy, in turn excites signal generation from neurons by a resonance mechanism to produce a burst (a dark soliton excitation) that shows up as a sharp wave ripple on the delta waveform, representing the transference of a memory copy.

Transient blocking signals may also play a role in REM sleep. There the signals are less energetic and have smaller range and consequently do not block visual and possibly auditory sensory pathways. If this is the case then the blocking signals co-produce the less energetic theta waveforms then their modulation by brain memory label frequencies in the frequency range $(10 - 16)$Hz, the analogue of sleep spindles, will make them look more like beta waves and the interaction between the theta waveforms and stored memory will stimulate and consolidate memories which are experienced as dreams. Thus dreaming should be a universal experience for all mammals. Just as a high energy blocking excitation shows up as a K-complex followed by sleep spindles on delta waveform modulation in NREM sleep, a less energetic blocking event should be present before the onset of REM. Perhaps they are the sawtooth wave modulation on theta waveforms observed (Suvadi 2015) before the onset of REM.

We were able to estimate the possible energy, range and durations of the wide variety of transient blocking signals that are theoretically possible. These theoretically allowed excitations have biological implications. They could be important, for example, for providing a mechanism for focused attention. Let us explain how. A low energy transient excitation would stop local access of certain signals thus permitting only signals of interest to be processed. At the same time the blocking excitation would generate its associated EEG waveforms that would be able to access locally stored memories labeled with frequencies that were shown to overlap with those of the EEG waveform generated. In this way relevant information from memory could be accessed by a

resonance process while information not of interest was blocked. Such a cooperative process would help explain aspects of attention. Thus two important related brain excitations happen together and cooperate.

There are further implications. Not only may the EEG waveforms help recall memory but they also may help to identify the nature of incoming signals as an incoming signal would, again generate an EEG waveform of a certain frequency which could, by the mechanism described, help to identify the nature of the incoming signal from stored memory. Furthermore, from the nature of the processes described, it also follows that EEG waveforms would also show up whenever focused attention is required, as it is natural to assume that a person can produces the low energy transient blocking signals required for attention, possibly by chemical means, to block signals that are not of interest and allow only certain signals to be processed.

Summarizing: soliton excitations carry information and store it as memory non locally, while transient blocking signals initiated by chemical means, of different energies, together with their co-produced EEG waveforms work together to carry out the cognitive functions of the brain. We suggest that EEG waveforms are the workhorse of cognitive activities and are the muscles of thinking. All our results follow from the topological and smoothness properties of a mathematical surface network that exactly captures the topological connectivity properties of a brain connectome.

Declarations

1. This research did not receive any specific grant from funding agencies in the public, commercial or not-for-profit sector.
2. The authors declare no competing financial interests.
3. Availability of data and methods (not applicable)
4. Code availability (not applicable)

Appendix A: Monodromy Groups and Tiling angles

The stable surface waves were shown to be special algebraic solutions of the linear hypergeoemetric equation and a way to co-produce them by pinch deformation excitations was described. Here we explain the link between monodromy groups, and tiling angles required to get the Schwarz solutions.

The hypergeometric equation solutions has two linearly independent solutions and its regular singular points, are chosen to be at $0, 1, \infty$. Each solution has characteristic exponents. Suppose b_0, b_1, b_∞ are the inverses of characteristic exponent differences of the hypergeometric differential equation near the singular points $0, 1, \infty$. We now recall that the hypergeometric equation can be written as,

$$x(1-x)\frac{d^2u}{dx^2} + (c-(a+b+1)\frac{du}{dx} - abu = 0$$

In terms of these parameters we have $\frac{1}{b_0} =$ 1-c, $\frac{1}{b_1} =$ c-a–b, $\frac{1}{b_\infty} =$ a-b, where the terms 1-c, c-a-b, a-b are the characteristic exponent differences of the given hypergeometric equation at its three singular points $x = 0, x = 1, x = \infty$ respectively.

The hypergeometric equation has an underlying group structure. It can be obtained as an eigenvalue equation of the Casimir operator of the Lie algebra $SL(2, C)$ (Miller 2010,Kitaev 2018). The group $SL(2, C)$ represents the symmetry of the sphere. Explicitly the group acts on a a point z of the upper half plane mapping it to a point w by $w = Mz$, where M is a 2×2 $SL(2, C)$ matrix with complex coefficients a, b, c, d as,

$$w = \frac{az + b}{cz + d}$$
$$ad - bc = 1$$

The hypergeometric functions also appear as the representaion of the Lie algebra of the group $SL(2, C)$ (Miller 2010) that is the symmetry of the Riemann sphere. The three regular singular points of the hypergeometric equation can be taken to be three points on a sphere. A curved triangle can be drawn on this sphere with these three points as its vertices. The spherical angles between the lines of this curved triangle are chosen to be associated to difference between characteristic exponents of the two linearly independent solutions of the hypergeometric equation at that regular singular point. Thus a solution, described by its characteristics has a geometric representation as a curved triangle on the surface of a sphere.

Fixing the tiling angles

The reason why differences of exponents appear in the analysis can be understood as follows: by analytic continuation (Yoshida 1987) a pair of linearly independent solutions can be extended to all points inside the triangle, the upper half plane and then, by using a reflection principle, (Yoshida 1987) to the lower half plane and thus extended to the entire sphere provided the characteristic exponents of the solutions are special. Such an extension can represent a tiling of the sphere.

Now consider the set $S = (0, 1, \infty)$ of the regular singular points of the hypergeometric differential equation and define $X = C^2 - S$, where C^2 is the two dimensional complex plane and x_0 a point in X. The hypergeometric differential equation has two linearly independent solutions, say u_1, u_2 in the neighborhood of a singular point. If we continue these solutions u_1, u_2 analytically along a curve C in X then we get

$$C^t_*(u_1, u_2) = M(C)^t(u_1, u_2)$$

where $M(C)$ is a non singular two-by-two matrix and C_* represents the analytic continuation of u_1, u_2 along the curve C. The matrices $M(C)$ for different curves forms a representation of the fundamental group of $\Pi(X, x_0)$ and is called the monodromy representation of the differential equation. The monodromy group representation for $\Pi(X, x_0)$ can be constructed from the characteristic exponents of the equations at its singular points. Explicitly if v_1, v_2 are the analytic continuations of u_1, u_2 we can write,

$$\begin{aligned} v_1 &= au_1 + bu_2 \\ v_2 &= cu_1 + du_2 \\ \frac{v_1}{v_2} &= \frac{au_1 + bu_2}{cu_1 + du_2} \\ &= \frac{a\frac{u_1}{u_2} + b}{c\frac{u_1}{u_2} + d} \\ ad - bc &= 1 \end{aligned}$$

Thus if $u_1 \approx z^\alpha, u_2 \approx z^\beta$ near a regular singular point, where α, β are characteristic exponents then the difference of the exponents appear naturally as parameters when we consider ratios of solutions. This is a projective way of studying the solutions. The mondodromy group has the as a linear fractional $PGL(2, c)$ transformation. It is a projective group.The group maps the ratio of appropriate solutions of the hyperheogeometric are real interval in the intervals $(0, 1), (0, \infty), (1, \infty)$. If we consider the strip of the upper half plane with $(0, 1)$ as the real axis then this strip is mapped to the curved triangle joining the point $0, \infty$ and $1, \infty$. The point ∞ is the north pole of the sphere. If such triangle has angles, given by the π(difference between critical exponents) in Schwarz list then by the action of the finite triangle subgroup of $PGL(2, C)$ these triangles tiles the upper half plane. Then by using a reflection principle of Schwarz (Yoshida 1987) this tiling can made to cover the entire sphere provided the spherical triangles have special angle values. Thus special solutions of the hypergeometric equation give a tiling of the sphere. The fact that the group of projective fractional linear transformations $PGL(2, C)$ maps circles and lines to circles and lines and preserves angles is used in the construction described.

The monodromy group $PGL(2, C)$ describes the way twists present at three specified singular points, given by the characteristic exponent differences, fit together. For the hypergeometric differential equation on the sphere this information completely fixes the solutions of the hypergeometric equation(Yoshida 1987).

References

[1] Arberello,E.(2001) Sketches of KdV, Contemporary Mathematics,312,9-70

[2] Atiyah(1971)M. Spin Structures. Ann.Scientifique de l'Ecole Normale Superieure, Quatrieme, Series, 4, 47-62
[3] Bievins.A.S.,Bassett.D,(2020),Topology in Biology,ISBN:978-3-319-70658-0
[4] R.Becker and G.Seldon(1985)The Body Electric, New York, Morrow, pages111-113,(1985)
[5] Bullock, T.H (1993) How do Brain Waves Work? Papers of a Neurophysiologist, Birhauser, Boston.
[6] Buzsaki G(1989), Two stage memory model: a role for noisy brain states, Neuroscience 31(3),551-570
[7] Buzsaki G(2015), Hippocampal sharp wave-ripple: a cognitive biomarker for episodic memory and planning, Hippocampus Oct 25 (10),1073-1085
[8] Colgin,L. et al (2009) Frequency of gamma oscillations routes flow of information in the hippocampus. Nature, 462, 353-357
[9] De Gannaro,L et al.(2003) Sleep Spindles: an Overview, Sleep Med Rev Oct 7(5) 423-40
[10] Curto.C,(2017)What can topology tell us about the neural code?,Bulletin of the AMS,54,63-78
[11] Lopez da Silva F.H (1991); Neural mechanisms underlying brain waves; from membranes to networks. Electroencephalography and Clinical Neurophysiology,79:81-93
[12] F.Lopez da-Silva (2010) EEG: Origin and Measurements, in EEG-fMRI, Springer Verlag Berlin Heidelberg
[13] K. Dharani(2015), Biology of Thought, Academic Press,109-122
[14] J. DeFilpe, et al.(1992) The pyramidal neuron of the cerebral cortex: morphological and chemical characteristcs of the synaptic inputs, Prog.in Neurobiology,39,563-607
[15] Fingelkurts A et al,(2014) EEG Oscillatory States: Universality,Uniqueness and Specificity across Healthy-Normal, Alterted and Pathological Brain Conditions, PLos One9(2),e87507
[16] Kanari.l,Dlotka.P,Scolamiero.M,Levi.R,Hess.K,Markram.H,(2018)A topological representation of branching neuronal morphologies,Neuroinformatics16,3-13
[17] Ioannides A(2019) The Emergence of Spindles and K-complexes and the role of the Dorsal Caudal partof the Anterior Cingulate as the generator of K-complexes.
[18] Harnack A(1876), Ueber die Vieltheiligkeit der ebenen algebraischen Curven,Math.Ann,10,189-199
[19] Hong S(2013) Dopamine System manager of neural pathways, Frontiers of Neuroscience v7 PMID 24367324
[20] Jones S et al.(2016) Neural mechanism of transient neocortical beta hythms: converging evidence from humans, computational modeling, monkeys and mice. PNAS:16041351113
[21] Kalla,C; Breathers and generalized non-linear Schroedinger equations as degenerations of algebro-geometric solutions, J.Phys.A: Math.Theor.44

(2011)

[22] KlimeschiW (2018) The frequency architecture of brain and brain-body oscillations: an analysis, Eu.J.Neuroscience 48(7),2431-2453

[23] Kalinchuk,A.,McCarley,R.,Porkka-Heiskanen,T.,Basheer,R.,(2010) Sleep Deprivation Triggers Inducible Nitric Oxide-Dependent Nitric Oxide Production in Wake-Active Basal Forbrain Neurons, The Journal of Neuroscience,30(40):13254-13264

[24] Kitaev A(2018); Notes on SL(2,R) representations, arXiv:1711.08169v2

[25] Kim,Yoo Sung.,Choi,J.,Yoon,Bo-Eun.,.(2020) Neuron-Glial Interactions in Neurodevelopment Disorder, Cell,Oct,9(10),2176

[26] Liu, Ning-Han (2013 Recognizing the Degree of Human Attention using EEG Signals for Mobile Sensors, Sensor(Basel) Aug, 10273-10286

[27] Maier R(2018); Associated Legendre Functions and Spherical Harmonics of Fractal Degree and Order; arXiv:1702.0855v3[math.CA]

[28] Marcolli.M,(2019),Gamma Spaces and Information,J.Geometric Physics,140,26-55

[29] Maya Geva-Sagiv, Yuval Nir,(2019) Local Sleep Oscillations: Implications for Memory Consolidation, Frontiers Nueroscience,13,813

[30] Miller W(2010) The Lie theory approach to Special Functions. University of Minnesta, November

[31] Morse,P and Feshbach, H Methods of Mathematical Physics,791, Chapter7, McGraw-Hill,(1953)

[32] Mumford D(1971) Ann.Scientifique del'Ecole Normale Superieure, Quatrieme, Series, 4,181-192

[33] Mumford D(1987) Tata Lectures onTheta,Chapter1,3

[34] Nash C, Sen S(1983) Topology and Geometry for Physicists, Academic Press

[35] Nunez P.L(2006a) The Neurophysics of EEG(2006) Second Edition, Oxford University Press

[36] Nunez P.L and Srinivasan(2006b) A theoretical basis for standing and traveling brain waves measured with human EEG with implications for integrated consciousness. Clinc Neurophysiol, 117(11),2424-2435

[37] Tomofumi Oga, et al(2016) Basal Dendrites of Layer 3, pyramidal neurons do not scale with change in cortical magnification in Macaque Primary Visual Cortex, (Fig 7), Frontiers Neuron Circuittes 10:74

[38] Reimann.M,Nolte.M,Scolamiero.M,Turner.K,Markram.H,(2017),Cliques of neurons bound into Cavities Provide a Missing Link between Structure and Function,Frontiers in Computational Neuroscience,Vol 11,art 48(6 pages)

[39] Ronveaux,A (Editor)(1995) Heun's Differential Equation, Oxford University Press

[40] Schwarz H(1873), Crelle Journal,75, 292-335

[41] Scott,A (2002) Neuroscience, A Mathematical Primer, Springer

[42] Sen S;Tomas Ryan,David Muldowney Maurizio Pezzoli (2021) Memory as a Topological Structure on a Surface Network (Under review Science

Reports).
[43] Suradi Y(2015) Sawtooth waves, Neurology;84,e87-e88
[44] T.Yamakawa (2018), Endogenous Nitric Oxide inhibits, whereas Awaking stimuli increase the Activity of a subset of Orexin neurons, Biological and Pharmaceutical Bulletin, 41, 12
[45] Vidunas R(2008), Transformation of algebraic Gaussian functions; arXiv-087.4808 [mathC.A]
[46] Vidunas R(2009), Funkcidaj Ekvacioj,139-180
[47] Weigenand,A.,Shellenberger Costa,M.,Ngo,Hong-Viet Victor.,Claussen,J.C.,.(2014), Characterization of K-complexes and Slow Wave Activity in a Neural Mass Model, PLOS Computational Biology, Nov 13 (2014)
[48] Wolfram MathWorld, Spherical Triangles
[49] Yoshida M(1987),Fuchsian Differential Equations.Friedr.Vieweg and Sohn

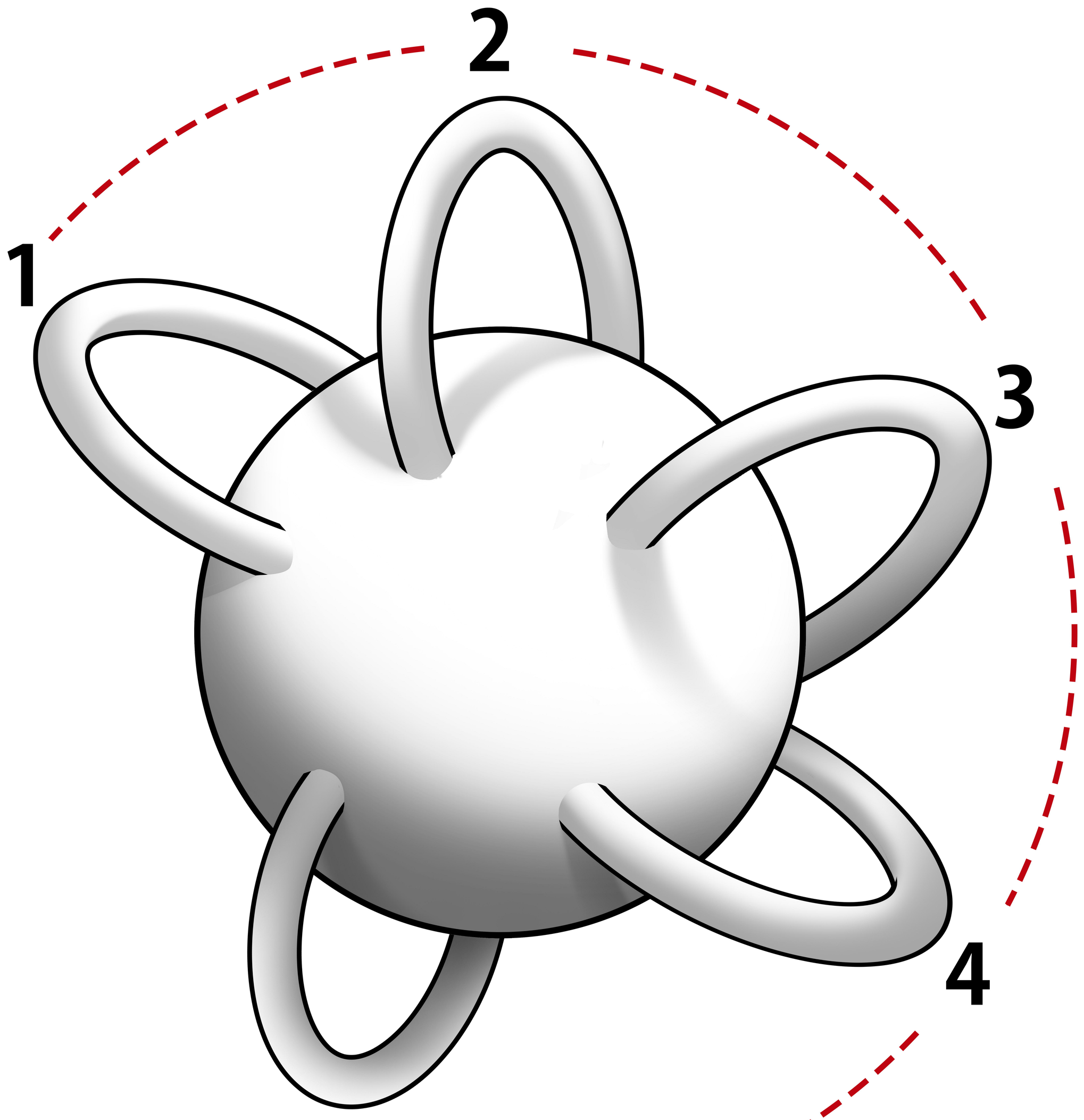
2
1
3
4
g

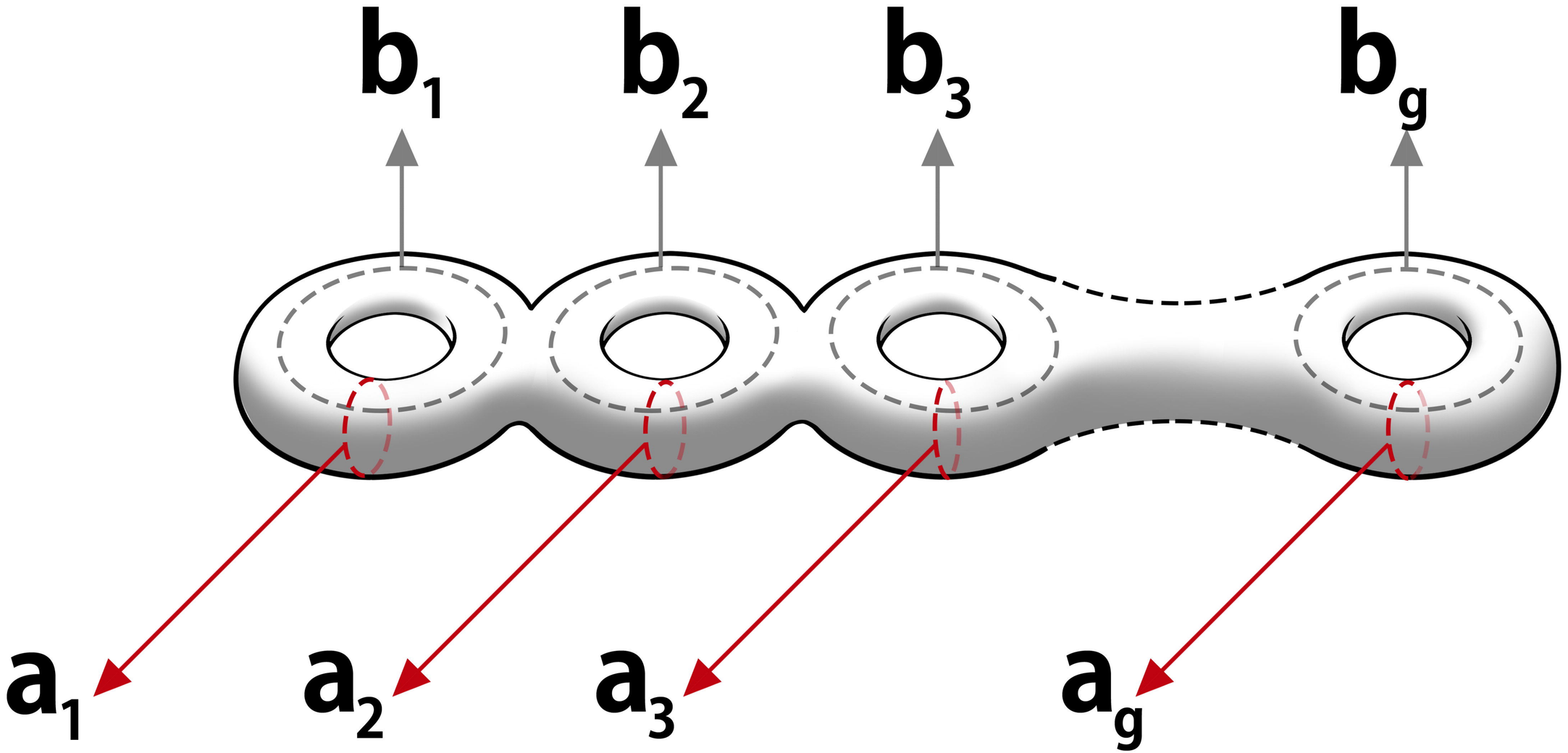
b_1
b_2
b_3
b_g
a_1
a_2
a_3
a_g

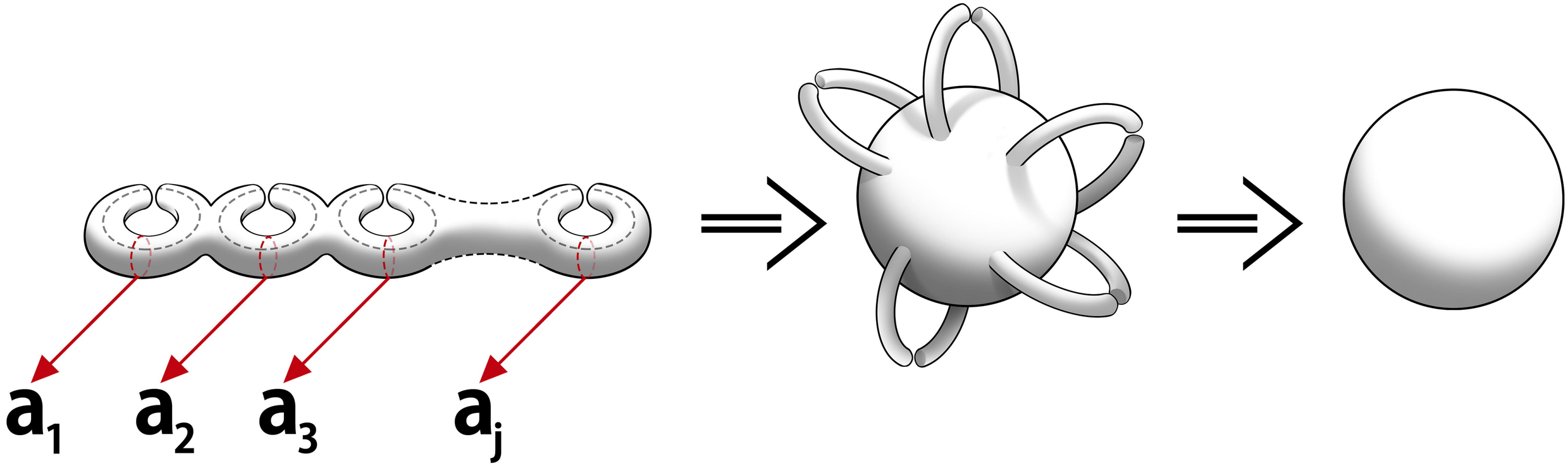
a_1
a_2
a_3
a_j

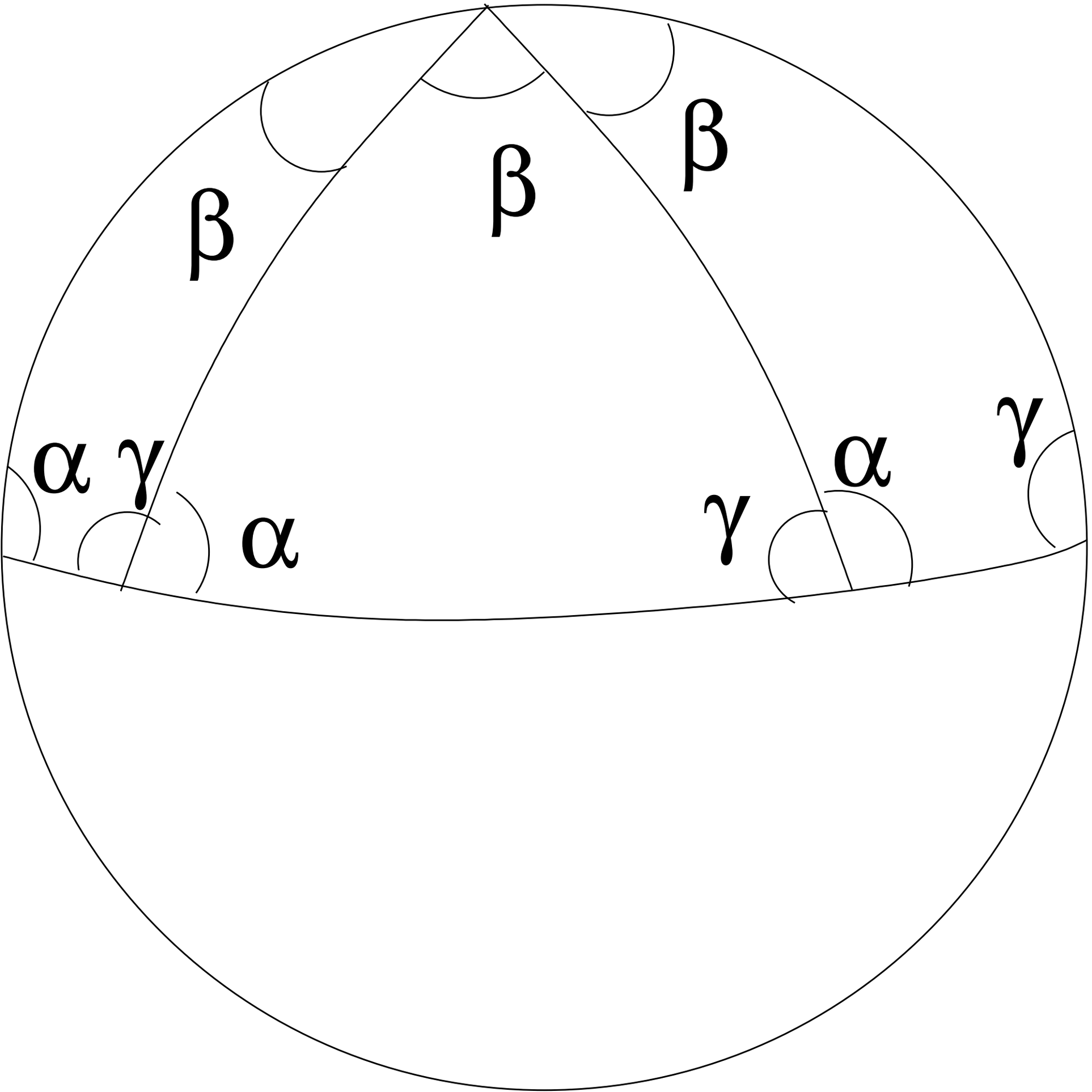
β
β
β
α
γ
α
γ
α
γ

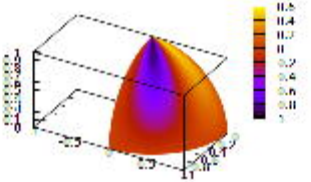

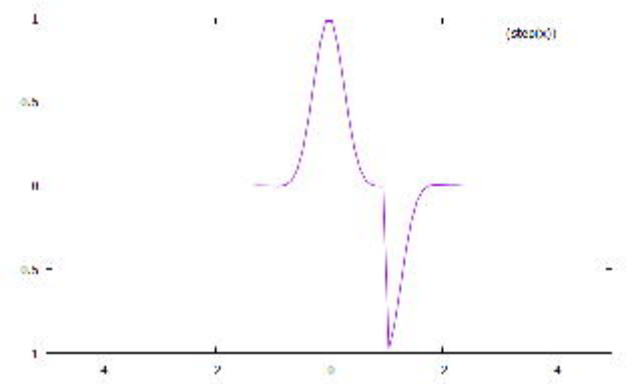
1
0.5
0
-0.5
-1
-4
-2
0
2
4

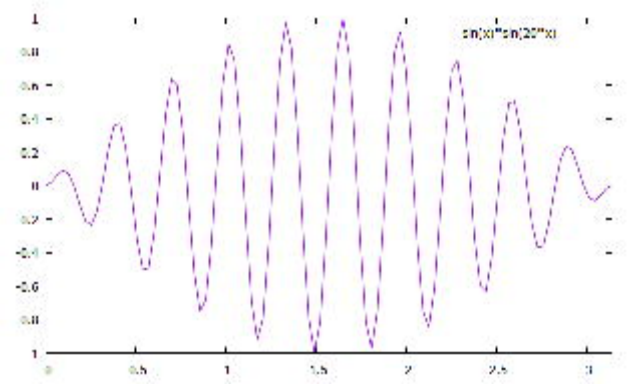
sin(x)*sin(25*x)
1
0.8
0.6
0.4
0.2
0
-0.2
-0.4
-0.6
-0.8
-1
0
0.5
1
1.5
2
2.5
3

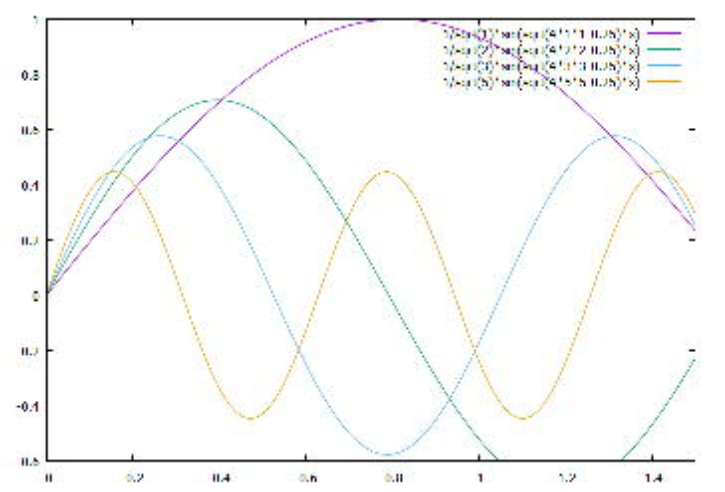
1/sqrt(1)*sin(sqrt(9.8*1)*1.0.05*x)
1/sqrt(2)*sin(sqrt(9.8*1)*2.0.05*x)
1/sqrt(3)*sin(sqrt(9.8*1)*3.0.05*x)
1/sqrt(5)*sin(sqrt(9.8*1)*5.0.05*x)
1
0.8
0.6
0.4
0.2
0
-0.2
-0.4
-0.6
0
0.2
0.4
0.6
0.8
1
1.2
1.4